invariant ϵ of the motion. The displacement invariants (c_1, b_2) appear only in the term D_0. This pattern is also true for all the loci as can be seen by examining Table 1.

The curves A_0 and D_0 are respectively the X axis and Y axis of V, and are independent of the invariants of the motion. The directions in the upper half plane have $\text{sgn}(\bar{A}) = +1$ for all motions since by definition ϵ is positive.

In the case of D_0, the right half plane has $\text{sgn}(\bar{D}) = +1$ when $(b_2 - 2c_1\epsilon) > 0$ and $\text{sgn}(\bar{D}) = -1$ in the left half plane; this situation is reversed when $(b_2 - 2c_1\epsilon) < 0$. The curve B_0 is a circle in the right half plane of V, tangent to the Y-axis at the origin, with a radius of ϵ. The directions inside B_0 have $\text{sgn}(\bar{B}) = -1$ those outside it have $\text{sgn}(\bar{B}) = +1$. Fig. 17 shows the distribution of $\text{sgn}(\bar{A}, \bar{B}, \bar{D})$ in V for $\epsilon = 1/2, b_2 = 1, c_1 = 1/2$.

It is interesting to notice that due to properties of the curves A_0, B_0, and D_0 the cases $\text{sgn}(\bar{A}, \bar{B}, \bar{D}) = (+, -, -)$ and $(-, -, -)$ cannot occur when $(b_2 - 2c_1\epsilon) > 0$. Similarly, when $(b_2 - 2c_1\epsilon) < 0$ it is the cases $\text{sgn}(\bar{A}, \bar{B}, \bar{D}) = (+, -, +)$ and $(-, -, +)$ which are excluded.

Using the equations in Table 1 it is possible to simply calculate, $\bar{A}$, $\bar{B}$, and $\bar{D}$ for each locus of equation (51). By plotting the line L_0 for each property P, K, P′ and K′ and defining the values of sgn(P, K, P′, K′) for the remaining lines in M, the shapes of each line trajectory parallel to a direction **e** can be described. Fig. 18 is an example of this description for lines in the moving body in the direction $\theta = 45°$ and $\psi = 22.5°$. The motion invariants used for this example are $\epsilon = 1/2$, $\gamma_x = 1/4$, $\gamma_y = 1/4$, and $c_1 = 1/2$, $b_2 = 1, c_2 = 0, a_3 = 1/2, b_3 = 1/4, c_3 = 0$. A figure such as this exists for each direction **e**.

It is interesting to note that in general there are 16 fundamental shapes of line trajectories to the third order, considering only the positional properties. Yet a general figure of four interesecting lines can define at most 11 regions. Thus, for any direction **e** at least 5 trajectory shapes are impossible.

It should be noted that our sign convention is such that in the cylindric-cylindric crank model the moving axis L (Fig. 16) points toward the positive Z half-space. The direction of L^1, the fixed axis, is such that ρ is always between 0 and 180°. By definition, the function P is positive when L^1 is located in the $-\mathbf{T}$ direction from L. Accordingly positive P implies that the fixed axis is on the same side of L as the screw axis Z (recall all three lines cut **T** at right angles), conversely a negative P implies L^1 and the screw axis are on opposite sides of L for lines in the upper half-plane of M. The opposite is true for lines in the lower half plane. The sign of P implies an increase of the crank length in the $-\mathbf{T}$ direction if P′ is positive and increase in the $+T$ direction if P′ is negative. Hence, for positive P′ and positive P the concavity of the ruled surface tends to reduce as we move along the surface toward the next ruling. In a similar way other sign combinations imply specific types of change in surface shape.

K is positive if this velocity is along the positive direction of the fixed axis L^1. A negative K′ implies an increase of velocity along this direction. The effect on the ruled surface of K and K′ is to determine how the point of closest approach of L and L^1 changes. The effect of K on the surface shape follows from Fig. 16.

Conclusions

The parameters called the instantaneous invariants provide a unique set of constants which identify a particular motion. The relation between the trajectories generated by the moving body and these constants can be obtained by studying the loci of moving elements which have special trajectory properties. These loci act as boundaries to regions with standard trajectory shapes, these boundaries depend directly upon the invariants of the motion.

In this paper the relationship between a motion and the trajectories it generates is studied to the third order for planar, spherical and spatial motions. The planar and spherical cases are seen to be very similar and a complete description of their point trajectories is possible, given their third order invariants. Spatial motion is distinctly different from these previous cases, yet by restricting attention to line trajectories the results of spherical kinematics may be applied directly to the directional characteristics of these trajectories.

Thus the additional aspects of spatial motion are only the positional characteristics, these are described by two functions P and K. The loci of lines whose trajectories have zero values for P and K, and their derivatives P′ and K′, are line complexes in the moving body. By examining one direction at a time and transforming coordinates so the lines in this direction are seen as points on a plane M, these loci appear as four lines in M. The regions in M of special trajectory shapes provide a description of spatial motion similar to that developed for planar and spherical motion. A method for extending this description to all directions of lines in the body is discussed briefly using the locus P = 0 as an example.

The purpose of this study is to provide a framework in which to understand the effect of the invariants on the trajectory shapes. Using these methods it is possible to distinguish qualitative differences between motions. Hence, we expect that these technqiues will be useful in both the analysis and synthesis of motion.

Acknowledgment

This material is based upon work supported by the National Science Foundation under grants NSF 75-21710 and NSF 79-10313.

References

1 Bottema, O., and Roth, B., *Theoretical Kinematics,* North Holland Publishing Co., 1979.

2 Dittrich, G., *Über die momentane Bewegungsgeometrie eines sphärisch bewegten starren Systems,* Dissertation, Aachen, 1964, 101 pp.

3 Kirson, Y., *Curvature Theory in Space Kinematics,* Ph.D. Dissertation, University of California at Berkeley, 1975.

4 McCarthy, J. M., *Instantaneous Kinematic Properties of Point and Line Trajectories,* Ph.D. Dissertation, Stanford University 1979.

5 McCarthy, J. M., and Roth, B., "The Curvature Theory of Line Trajectories in Spatial Kinematics," ASME JOURNAL OF MECHANICAL DESIGN, Vol. 103, No. 4, Oct. 1981, pp. 718–724.

6 Veldkamp, G., R., *Curvature Theory in Plane Kinematics,* Dissertation Technical University of Delft, 1963.

DISCUSSION

K. H. Hunt.[1] The authors present an interesting approach to categorizing the shapes of trajectories. Here I confine my remarks to trajectories of lines in spherical motion.

While I accept that Fig. 15 is meant as no more than an example of categories of line-trajectories, represented as projections on a plane of points on the surface of a sphere, it is perhaps a pity that the regions are incomplete. The plane of projection in Fig. 10 would need to be of infinite extent to include an entire hemisphere. Only one ball-axis is

[1] Prof. of Mechanism, Dept. of Mechanical Engineering, Monash University, Clayton, Victoria, Australia.

represented, whereas there can be as many as four. The two cubic cones (of inflection and stationary curvature) might be expected to have nine lines in common, but in that event three of the lines coalesce along the instantaneous rotational axis and two are always imaginary. Accordingly, the "+ −" region in the first quadrant is bounded, and a further region exists beyond it. Moreover, the relative proportions of the two cubics could have been chosen to show two more real ball-axes and hence two more bounded regions.

Even though drafting difficulties would be introduced, three-dimensional views of the cones (along the lines of Figs. 14.2 and 14.4 in [7]) would in my opinion have been preferable.

It is noteworthy that for four finitely separated locations in spherical motion there can be as many as six real lines analogous to ball-axes. However, when the location separation is infinitesimal two of these lines become imaginary (see [7], p. 412, where other sources are also quoted). In early kinematic researches this reduction from six to four was not appreciated ([7], p. 407), and it is important to avoid perpetuating any possible misconception on this matter.

Additional References

[7] Hunt, K. H., *Kinematic Geometry of Mechanisms,* Clarendon Press, Oxford, 1978.

Authors' Closure

We thank Professor Hunt for his comments, and in accordance with his wishes present a discussion of the case when there are four real Ball lines.

Ball's lines in spherical kinematics can be obtained as the lines of intersection of the cubic cones γ_0 and γ_0' (equations (21) and (22), respectively). These cones have nine lines of intersection, but three are trivial, since they occur along the z-axis ($x = y = 0$), and two are always imaginary. This leaves at most four other real lines of intersection, and these are the lines we call the Ball lines.

Our purpose here is to determine for which motions there are four real Ball lines. It is simplest to do this by studying the plane curves $\bar{\gamma}_0$ and $\bar{\gamma}_0'$ (equations (24) and (25)) which are obtained by intersecting the cubic cones with the plane $Z = 1$. The problem then becomes one of determining when the two circular cubics $\bar{\gamma}_0$ and $\bar{\gamma}_0'$ have four real intersections (other than those at the origin).

We transform (24) and (25) into polar coordinates and eliminate the polar angle between these two equations. It then follows that the radial distances, r, of the nontrivial intersections are the roots of the following quartic in r^2.

$$c_0(r^2)^4 + c_1(r^2)^3 + c_2(r^2)^2 + c_3(r^2) + c_4 = 0$$

where

$$c_0 = \epsilon^2\beta^2$$

$$c_1 = \beta(4\epsilon^2\beta - 6\epsilon^3 - \beta - \gamma_y^2)$$

$$c_2 = (\beta - 3\epsilon)^2\epsilon^2 + 2\beta(\beta - 3\epsilon)(2\epsilon^2 - 1) + \beta^2\epsilon^2 - 2\gamma_y^2$$

$$c_3 = (\beta - 3\epsilon)^2(2\epsilon^2 - 1) + 2\beta(\beta - 3\epsilon)\epsilon^2 - \gamma_y^2$$

$$c_4 = (\beta - 3\epsilon)^2\epsilon^2$$

and

$$\beta = \frac{3}{2}\epsilon + \gamma_x.$$

Since c_0 and c_4 are always positive, it follows that it is necessary that $c_1 < 0$, $c_2 > 0$, $c_3 < 0$ if we are to have four positive real roots of r^2 and hence real values for r.

From Fig. 12 it follows that $\gamma_x > -3/2\,\epsilon$ is required. Also, in order that C_x (equation (29)) have a greater diameter than the circle of curvature of γ_0, we must have $\gamma_x < 3/2\,\epsilon$. Figure 11 suggests that ϵ must be less than 1/2, therefore $-3/4 < \gamma_x < 3/4$. These conditions guarantee that $c_1 < 0$ and $c_3 < 0$. An upper bound on γ_y then follows from the condition $c_2 > 0$; since only γ_y^2 enters into our equations the lower bound is the negative of the positive upper bound.

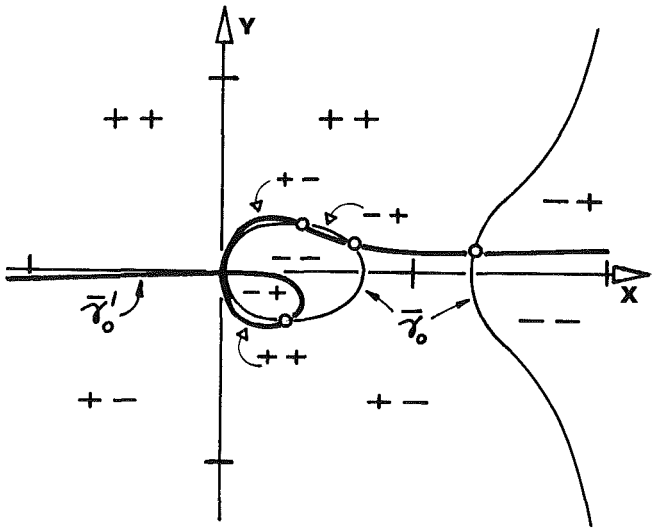

Fig. 19 Example of the third order representation of point trajectory shapes for a spherical motion with $\epsilon = 0.480$, $\gamma_x = 0.500$, $\gamma_y = 0.038$. The ordered pairs of signs are those of γ and γ', respectively.

Although the condition $c_2 > 0$ is necessary it is not sufficient; to obtain the sufficient condition for four real Ball lines we need to use the value of γ_y which makes the discriminant of the quartic equation vanish. The upper bound of γ_y is obtained from

$$(c_0c_4 - 4c_1c_3 + 3c_2^2)^3 - 27(c_0c_2c_4 - c_0c_3^2 - c_1^2c_4 + 2c_1c_2c_3 - c_2^3)^2 = 0.$$

Figure 19 shows an example of four real Ball lines; the third order properties are denoted and can be compared to the example shown in Fig. 15.

In Fig. 19, $\epsilon = 0.480$, $\gamma_x = 0.500$, and $\gamma_y = 0.038$. For these values of ϵ and γ_x the upper bound for γ_y is 0.2067, as determined from the discriminant. Hence, for $\epsilon = 0.480$, $\gamma_x = 0.500$ four real Ball lines will exist for all spherical motions for which $-0.2067 \leq \gamma_y \leq 0.2067$.